Polyhedron 34 (2012) 129–135

Contents lists available at SciVerse ScienceDirect

Polyhedron

journal homepage: www.elsevier.com/locate/poly

The structural diversity and luminescent properties of Zn(II) coordination assemblies with cyclohexane (or cyclohexene) dicarboxylate anions and two positional isomeric ligands

Fu-Ping Huang [a,b], Jing-Bin Lei [a], Qing Yu [a], He-Dong Bian [a,*], Shi-Ping Yan [b,*]

[a] *Key Laboratory for the Chemistry and Molecular Engineering of Medicinal Resources, Department Chemistry and Chemical Engineering, Guangxi Normal University, Ministry of Education of China, Guilin 541004, PR China*

[b] *Department of Chemistry, Nankai University, Tianjin 300071, PR China*

A R T I C L E   I N F O

Article history:
Received 4 November 2011
Accepted 17 December 2011
Available online 8 January 2012

Keywords:
Zn(II) coordination polymers
Positional isomeric ligands
Luminescence properties

A B S T R A C T

Four Zn(II) coordination polymers, namely $\{[Zn(chedc)(4,4'\text{-}Hbpt)]\}_n$ (**1**), $\{[Zn_3(chadc)_2(4,4'\text{-}Hbpt)_2(4,4'\text{-}bpt)_2]\cdot 3H_2O\}_n$ (**2**), $\{[Zn_2(chadc)_2(3,3'\text{-}Hbpt)]\}_n$ (**3**) and $\{[Zn_2(chedc)_2(3,3'\text{-}Hbpt)]\cdot H_2O\}_n$ (**4**) (chadc = *cis*-1,2-cyclohexanedicarboxylate anion, chedc = *cis*-4-cyclohexene-1,2-dicarboxylate anion, 4,4′-Hbpt = 1H-3,5-bis(4-pyridyl)-1,2,4-triazole, 3,3′-Hbpt = 1H-3,5-bis(3-pyridyl)-1,2,4-triazole) have been produced by the reaction of two positional isomeric dipyridyl bridging ligands and two dicarboxylate anions with Zn(II) salts under hydrothermal conditions. Structural analysis reveals that **1** exhibits a double-chain and **2** exhibits a 3D network with a $(6^2.10)_2(6^4.10^2)$ topology, whilst **3** and **4** show similar layer structures. The luminescent properties of these complexes have been briefly investigated.

1. Introduction

The design and construction of coordination polymers is of current interest in the field of crystal engineering not only for their intriguing variety of architectures and topologies but also for their tremendous potential application in luminescence, catalysis, nonlinear optics, gas adsorption, magnetism, and medicine [1,2]. However, it is still a great challenge to rationally prepare and predict their exact structures. Generally, many factors can affect the structures of the final products, such as counter anions [3], the pH values of the reaction solutions [4], temperature [5], molar ratio between reactants [6] and solvent system [7]. One of the most useful and important way of studying the controllable synthesis of the molecular architecture is still the reasonable choice of well-designed organic ligands as bridges or terminal groups (building blocks) with metal ions or clusters as nodes, and many strategies have already been developed based on previous works [8,9]. The selection of the ligands plays a key role because deliberate modifications on the organic ligands can dramatically influence the ultimate structural topologies of the coordination solids [10,11].

In the last few years, through introducing the 1H-1,2,4-triazole moiety between a couple of 4-pyridyl (or 3-pyridyl) groups, we have designed three positional isomeric *N*,*N*′-donor ligands: 1H-3,5-bis(4-pyridyl)-1,2,4-triazole (4,4′-Hbpt), 1H-3-(3-pyridyl)-5-(4-pyridyl)-1,2,4-triazole (3,4′-Hbpt) and 1H-3,5-bis(3-pyridyl)-1,2,4-triazole (3,3′-Hbpt) (Chart 1), and a series of interesting coordination polymers have been synthesized and structurally characterized [12,13]. The different positions of the pyridyl N atoms in the positional isomeric ligands may benefit the formation of different topological structures, which are very useful in supramolecular chemistry, crystal engineering and design [14]. As a part of this ongoing work, we present here the structural diversity and luminescent properties of four Zn(II) complexes: $\{[Zn(chedc)(4,4'\text{-}Hbpt)]\}_n$ (**1**), $\{[Zn_3(chadc)_2(4,4'\text{-}Hbpt)_2(4,4'\text{-}bpt)_2]\cdot 3H_2O\}_n$ (**2**), $\{[Zn_2(chadc)_2(3,3'\text{-}Hbpt)]\}_n$ (**3**) and $\{[Zn_2(chedc)_2(3,3'\text{-}Hbpt)]\cdot H_2O\}_n$ (**4**) (where chadc = *cis*-1,2-cyclohexanedicarboxylate anion, chedc = *cis*-4-cyclohexene-1,2-dicarboxylate anion). In addition, the luminescent properties of these compounds have been investigated.

2. Experimental

2.1. Materials and physical measurements

With the exception of the ligands 4,4′-Hbpt and 3,3′-Hbpt, which were prepared according to the literature procedure [15], all reagents and solvents for the syntheses and analyses were commercially available and used as received. IR spectra were taken on a Perkin-Elmer spectrum One FT-IR spectrometer in the 4000–400 cm^{-1} region with KBr pellets. Elemental analyses for C, H and N were carried out on a Model 2400 II, Perkin-Elmer elemental

---

[*] Corresponding authors.
E-mail address: gxnuchem312@yahoo.com.cn (H.-D. Bian).

0277-5387/$ - see front matter © 2012 Elsevier Ltd. All rights reserved.
doi:10.1016/j.poly.2011.12.030

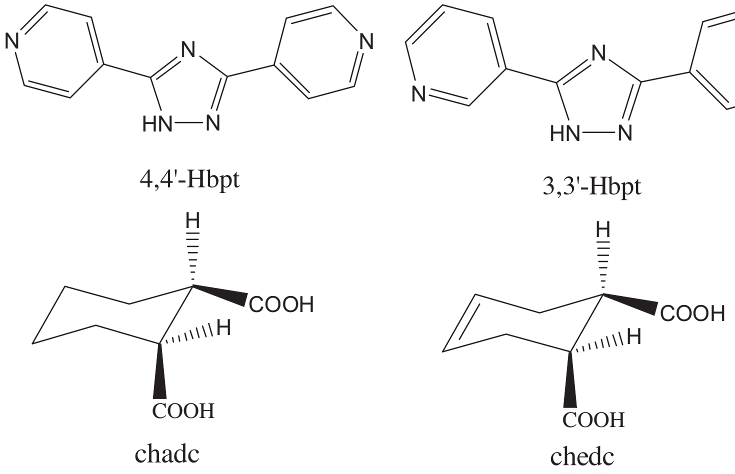

Chart 1. The ligands used in this work.

analyzer. Steady state fluorescence measurements were performed using an FL3-P-TCSPC fluorescence spectrofluorometer at ambient temperature in the solid-state.

2.2. Synthesis of {[Zn(chedc)(4,4′-Hbpt)]}$_n$ (**1**)

A mixture containing $Zn(CH_3COO)_2·2H_2O$ (110 mg, 0.5 mmol), 4,4′-Hbpt (112 mg, 0.5 mmol), chedc (85 mg, 0.5 mmol), NaOH (40 mg, 1 mmol), water (10 mL) and ethanol (3 mL) was sealed in a Teflon-lined stainless steel vessel (23 mL), which was heated at 120 °C for 3 days and then cooled to room temperature at a rate of 5 °C/h. Colorless block crystals of **1** were obtained and picked out, washed with distilled water and dried in air. *Anal.* Calc. for $C_{20}H_{17}ZnN_5O_4$: C, 52.54; H, 3.72; N, 15.32. Found: C, 52.78; H, 3.54; N, 15.74%. IR (KBr, cm^{-1}): 3423.07w, 3027w, 2829.67m, 1621.41s, 1562.79s, 1436.63m, 1330.61w, 1028.84w, 993.18w, 847.78w, 604.15w.

2.3. Synthesis of {[Zn_3(chadc)$_2$(4,4′-Hbpt)$_2$(4,4′-bpt)$_2$]·$3H_2O$}$_n$ (**2**)

The same synthetic procedure as that for **1** was used except that chedc was replaced by chadc, giving colorless block X-ray-quality crystals of **2**. *Anal.* Calc. for $C_{64}H_{60}Zn_3N_{20}O_{11}$: C, 51.83; H, 4.05; N, 18.90. Found: C, 51.27; H, 3.98; N, 18.68%. IR (KBr, cm^{-1}): 3441.29m, 3032.96m, 2934.06m, 1616.61s, 1566.54s, 1449.93s, 1220.88m, 1028.84w, 998.67w, 842.30m, 737.14m.

2.4. Synthesis of {[Zn_2(chadc)$_2$(3,3′-Hbpt)]}$_n$ (**3**)

The same synthetic procedure as that for **2** was used except that 4,4′-Hbpt was replaced by 3,3′-Hbpt, giving colorless block X-ray-quality crystals of **3**. *Anal.* Calc. for $C_{28}H_{29}Zn_2N_5O_8$: C, 48.39; H, 4.18; N, 10.08. Found: C, 48.56; H, 4.43; N, 10.14%. IR (KBr, cm^{-1}): 3434.06m, 3082m, 2941.01s, 1604.62s, 1446.05s, 1426.63s, 1198.93w, 1053.53w, 979.46w, 842.30w, 697.13m.

2.5. Synthesis of {[Zn_2(chedc)$_2$(3,3′-Hbpt)]·H_2O}$_n$ (**4**)

The same synthetic procedure as that for **1** was used except that 4,4′-Hbpt was replaced by 3,3′-Hbpt, giving colorless block X-ray-quality crystals of **4**. *Anal.* Calc. for $C_{28}H_{27}Zn_2N_5O_9$: C, 47.44; H, 3.81; N, 9.88. Found: C, 47.05; H, 3.76; N, 9.96%. IR (KBr, cm^{-1}): 3434.06m, 3065.93m, 2921.95m, 1605.84s, 1421.08s, 1358.05w, 1220.88m, 1056.28w, 993.18w, 812.12m, 697.28m.

2.6. X-ray crystallography

X-ray single-crystal diffraction data for **1–4** were collected with a Bruker SMART CCD instrument using graphite monochromatic Mo Kα radiation (λ = 0.71073 Å). The data were collected at 293(2) K and there was no evidence of crystal decay during data collection. A semi-empirical absorption correction was applied using SADABS and the program SAINT was used for integration of the diffraction profiles [16]. The structures were solved by direct methods with the program SHELXS-97 and refined by full-matrix least-squares methods on all F^2 data with SHELXL-97 [17]. The non-hydrogen atoms were refined anisotropically. Hydrogen atoms of water molecules were located in a difference Fourier map and refined isotropically in the final refinement cycles. Other hydrogen atoms were placed in calculated positions and refined using a riding model. The final cycle of full-matrix least-squares refinement was based on observed reflections and variable parameters. Further crystallographic data and structural refinement details are summarized in Table 1. Selected bond lengths and bond angles are given in Table 2.

3. Results and discussion

3.1. Structural description of **1–4**

3.1.1. {[Zn(chedc)(4,4′-Hbpt)]}$_n$ (**1**)

Complex **1** is an infinite 1-D polymer with a double-chain structure. The asymmetric unit of **1** consists of one Zn(II) cation, one 4,4′-Hbpt molecule and one chedc anion (Fig. 1(a)). The Zn(II) ions exhibit a distorted tetrahedral environment with two carboxylic O atoms from two chedc anions [Zn1–O1 = 1.967(2) Å; Zn1–O3A = 1.955(19) Å] and two N atoms from two 4,4′-Hbpt ligands [Zn1–N1 = 2.044(2) Å; Zn1–N5B = 2.049(2) Å]. As illustrated in Fig. 1(b), the 4,4′-Hbpt ligands bridge adjacent Zn(II) ions to form a 1-D chain running along the *a*-axis. Two single [Zn(4,4′-Hbpt)] chains are further combined by two carboxylic groups of chedc to form a double-chain. The Zn···Zn distance separated by the 4,4′-Hbpt linker is 13.763(3) Å, and it is 5.146(1) Å in the dimeric unit bridged by a pair of carboxylate groups.

A 3D supramolecular structure (Fig. 1(d)) is constructed by hydrogen bonding interactions between the triazole N atoms from 4,4′-Hbpt and the carboxylate oxygen atoms from $(chedc)^{2-}$ anions [N2–H2A···O2#1, symmetry codes: (#1) $x + 3/2$, $y + 1/2$, $z + 1$]. Therefore, hydrogen bonding interactions play an important role in stabilizing the supramolecular structures.

Table 1
Crystal data and structure refinement for **1**–**4**.

Complex	**1**	**2**	**3**	**4**
Empirical formula	$C_{20}H_{17}N_5O_4$ Zn	$C_{64}H_{60}N_{20}O_{11}Zn_3$	$C_{28}H_{29}N_5O_8Zn_2$	$C_{28}H_{27}N_5O_9Zn_2$
Formula weight (*M*)	456.78	1481.49	694.34	708.33
Crystal system	monoclinic	monoclinic	monoclinic	monoclinic
Space group	*C*2/*c*	*C*2/*c*	$P2_1/c$	$P2_1/c$
a (Å)	22.388(5)	35.823(7)	7.0490(1)	7.1260(1)
b (Å)	13.763(3)	9.810(2)	18.214(4)	18.309(4)
c (Å)	15.079(3)	25.171(5)	21.185(4)	21.127(4)
β (°)	124.35(3)	129.14(3)	91.28(3)	93.32(3)
V ($Å^3$)	3835.9(2)	6861(2)	2719.3(9)	2751.8(9)
Z	8	4	4	4
D_{calc} (g/cm^3)	1.582	1.434	1.696	1.710
F(000)	2496	3048	1768	1768
θ Range for data collection (°)	3.11–27.48	3.02–25.00	3.09–25.50	3.07–25.25
Reflections collected/unique	18754/4367 [R_{int} = 0.0429]	17962/5985 [R_{int} = 0.1174]	23012/5051 [R_{int} = 0.0559]	13764/4804 [R_{int} = 0.0779]
Goodness-of-fit (GOF) on F^2	1.175	1.090	1.028	1.042
Final *R* indices [$I > 2\sigma(I)$]	$R_1 = 0.0471$ $\omega R_2 = 0.0837$	$R_1 = 0.1014$ $\omega R_2 = 0.2194$	$R_1 = 0.0523$ $\omega R_2 = 0.1260$	$R_1 = 0.0897$ $\omega R_2 = 0.1825$
R indices (all data)	$R_1 = 0.0644$ $\omega R_2 = 0.0885$	$R_1 = 0.1584$ $\omega R_2 = 0.2517$	$R_1 = 0.0777$ $\omega R_2 = 0.1372$	$R_1 = 0.1219$ $\omega R_2 = 0.1999$

Table 2
Selected bond lengths (Å) and bond angles (°) for **1**–**4**.

1 *(Symmetry codes: for **1**, A −x + 1/2, −y + 1/2, −z + 1; B x, y + 1, z.)*

Zn1–O1	1.967(2)	Zn1–N1	2.044(2)
Zn1–O3A	1.955(2)	Zn1–N5B	2.049(2)
O1–Zn1–N1	105.29(9)	O3A–Zn1–N1	95.49(9)
O1–Zn1–N5B	110.63(9)	O3A–Zn1–N5B	106.47(9)
O3A–Zn1–O1	114.22(8)	N1–Zn1–N5B	124.19(9)

2 *(Symmetry codes: for **2**, A −x + 1/2, y − 1/2, −z + 1/2; B −x + 1/2, −y + 1/2, −z; C x − 1/2, −y + 1/2, z − 1/2; D −x, y, −z − 1/2.)*

Zn1–O1	1.910(6)	Zn1–N1	2.068(7)
Zn1–N9	2.012(7)	Zn2–O3B	1.947(6)
Zn1–N10A	2.046(6)	Zn2–N6	2.039(7)
O1–Zn1–N9	105.7(3)	O3B–Zn2–O3C	115.2(4)
O1–Zn1–N10A	122.9(3)	O3B–Zn2–N6	96.9(3)
N9–Zn1–N10A	104.4(3)	O3C–Zn2–N6	121.2(3)
O1–Zn1–N1	110.6(3)	N6–Zn2–N6D	106.8(4)
N9–Zn1–N1	114.0(3)		
N10A–Zn1–N1	99.5(3)		

3 *(Symmetry codes: for **3**, A x − 1, y, z; B x − 1, −y + 1/2, z − 1/2; C x + 1, y, z.)*

Zn1–O5A	1.920(3)	Zn2–O1C	1.925(3)
Zn1–O2	1.944(3)	Zn2–O6	1.928(3)
Zn1–O7	1.955(3)	Zn2–O3	2.029(3)
Zn1–N5B	2.072(4)	Zn2–N1	2.075(4)
Zn1–O8	2.461(4)	Zn2–O4	2.325(4)
O5A–Zn1–O2	124.41(2)	O1C–Zn2–O6	127.46(2)
O5A–Zn1–O7	117.73(2)	O1C–Zn2–O3	114.36(2)
O2–Zn1–O7	114.14(2)	O6–Zn2–O3	115.48(2)
O5A–Zn1–N5B	93.82(1)	O1C–Zn2–N1	93.08(1)
O2–Zn1–N5B	98.43(1)	O6–Zn2–N1	98.04(1)
O7–Zn1–N5B	97.13(2)	O3–Zn2–N1	95.11(1)
O5A–Zn1–O8	92.20(1)	O1C–Zn2–O4	93.19(1)
O2–Zn1–O8	99.76(1)	O6–Zn2–O4	98.48(13)
O7–Zn1–O8	57.09(1)	O3–Zn2–O4	58.93(12)
N5B–Zn1–O8	153.00(1)	N1–Zn2–O4	153.46(13)

4 *(Symmetry codes: for **4**, A x − 1, y, z; B x, −y + 3/2, z + 1/2.)*

Zn1–O1	1.945(6)	Zn2–O2	1.929(6)
Zn1–O7A	1.956(6)	Zn2–O8A	1.930(6)
Zn1–N5B	2.052(7)	Zn2–O6	1.976(7)
Zn1–O4A	2.171(7)	Zn2–N1	2.071(7)
Zn1–O3A	2.181(7)	Zn2–O5	2.383(9)
O1–Zn1–O7A	130.3(3)	O2–Zn2–O8A	124.0(3)
O1–Zn1–N5B	93.8(3)	O2–Zn2–O6	115.8(3)
O7A–Zn1–N5B	95.2(3)	O8A–Zn2–O6	117.4(3)
O1–Zn1–O4A	94.1(3)	O2–Zn2–N1	97.8(3)
O7A–Zn1–O4A	100.6(3)	O8A–Zn2–N1	93.6(3)
N5B–Zn1–O4A	151.2(3)	O6–Zn2–N1	95.2(3)
O1–Zn1–O3A	112.1(3)	O2–Zn2–O5	102.2(3)
O7A–Zn1–O3A	116.3(3)	O8A–Zn2–O5	92.2(3)
N5B–Zn1–O3A	92.0(3)	O6–Zn2–O5	57.4(3)
O4A–Zn1–O3A	59.5(2)	N1–Zn2–O5	151.1(3)

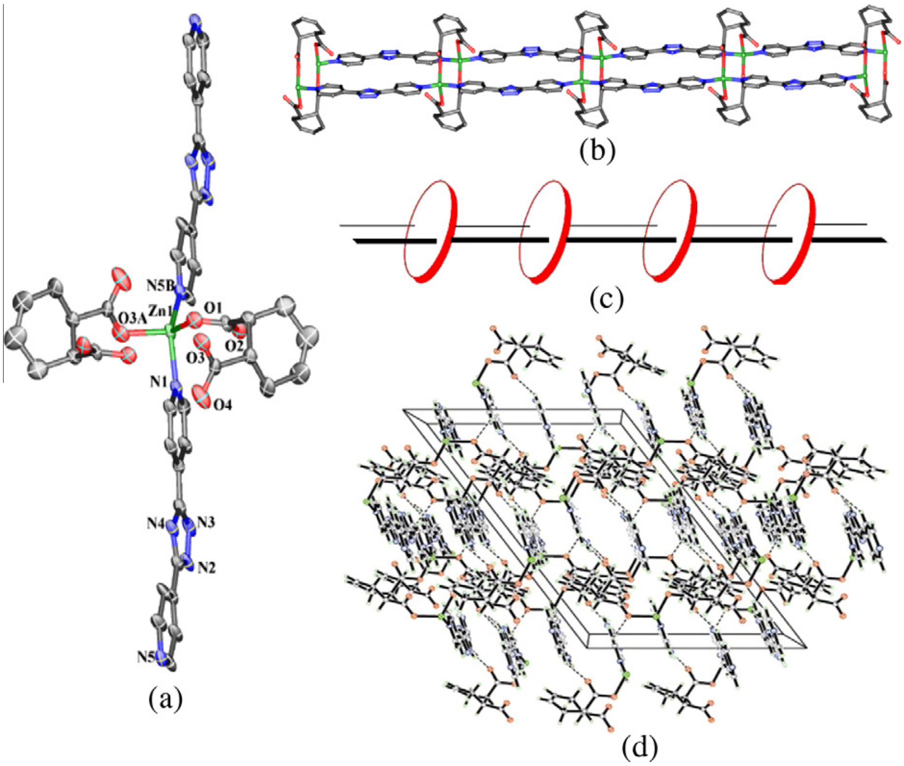

Fig. 1. (a) Structure of **1** showing the local coordination environments of the Zn(II) atoms; (b) the 1-D {[Zn(chedc)(4,4′-Hbpt)]}$_n$ chain; (c) the simple form of 1-D {[Zn(chedc)(4,4′-Hbpt)]}$_n$ chain; (d) a view of the crystal packing of **1** along the *a* axis.

3.1.2. {[Zn_3(chadc)$_2$(4,4′-Hbpt)$_2$(4,4′-bpt)$_2$]·3H_2O}$_n$ (**2**)

The asymmetric unit of **2** consists of one and a half Zn(II) ions, one 4,4′-Hbpt molecule, one 4,4′-bpt anion, one independent chadc anion, and one and a half lattice water molecules. As shown in Fig. 2(a), Zn1 takes a distorted tetrahedral geometry via coordinating to one carboxylic O atom of chadc [Zn1–O1 = 1.910(6) Å], two N atoms of two 4,4′-Hbpt ligands and one N atom of the 4,4′-bpt ligand [Zn1–N10A = 2.046(6) Å, Zn1–N1 = 2.068(7) Å, Zn1–N9 = 2.012(7) Å], whereas the Zn2 ion is located on a crystallographic 2-fold axis and displays a similar distorted tetrahedral environment, which is provided by two carboxylic O atoms from two chedc anions [Zn2–O3B = 1.947(6) Å] and two N atoms from two 4,4′-bpt ligands [Zn2–N6 = 2.039(7) Å].

It is interesting that 4,4′-Hbpt and 4,4′-bpt coexist in **2**, and they adopt two types of coordination modes (Scheme 1). As is shown in Fig. 2(a), one 4,4′-Hbpt ligand coordinates to Zn1 in a monodentate mode, with one uncoordinated pyridyl end (N5) dangling in the free space. The other 4,4′-bpt ligand acts as a μ_3-bridge, which connects the adjacent Zn1 through N9 and N10 resulting in a 1-D array, and further connects the Zn2 ions through N6 thus forming a 2-D polymeric layer, in which the Zn1···Zn2 distance separated by 4,4′-bpt is 9.773(2) Å. (Fig. 2(b)). Additionally, the two carboxylic groups of chadc, that all adopt a monodentate mode, connect with these zinc atoms to give a very complicated 3D network architecture (Fig. 2(c)). The packing shows guest water molecules O6 and O7 located inside tubular channels running down the *c* axis.

A better insight into the nature of this intricate architecture can be achieved by topological analysis. In **2**, on the basis of the connectivity of the Zn1 and Zn2 atoms, both of them are viewed to be 3-connected and 4-connected nodes, respectively. Moreover, according to Wells' topology definition [18], this 3D network can be further simplified by considering each 4,4′-bpt ligand as a 3-connected node. Therefore, the overall structure of **2** is a binodal (3,4)-connected net with Schläfli symbol of $(6^2.10)_2(6^4.10^2)$ [19], as depicted in Fig. 2(e). To the best of our knowledge, binodal (3,4)-connected metal–organic networks constructed by mixed ligands have rarely been reported [19]. It should be noted that the (3,4)-connected network in **2** is a new type, which is different from other (3,4)-connected nets, for example, the coordination net with a $(4.8^2)(4.8^2.10^3)$ topology [20]. This result may offer new insights into the controlled assembly of coordination solids.

3.1.3. {[Zn_2(chadc)$_2$(3,3′-Hbpt)]}$_n$ (**3**) and {[Zn_2(chedc)$_2$(3,3′-Hbpt)]·H_2O}$_n$ (**4**)

Single crystal X-ray diffraction analysis reveals that the crystal structures of complexes **3** and **4** are very similar, except that one chadc in **3** is replaced by chedc in **4**. As a result, only the structure of **3** is discussed in detail herein. Complex **3** presents a layered network in which the Zn(II) centers are bridged by 3,3′-Hbpt and chadc ligands. The asymmetric unit of **3** consists of two Zn(II) cations (Fig. 3(a)), one independent 3,3′-Hbpt molecule and two chadc anions. Both crystallographically independent Zn(II) atoms are surrounded by one N atom from a 3,3′-Hbpt ligand [Zn1–N5B = 2.072(4) Å; Zn2–N1 = 2.075(4) Å] and four O atoms from three chadc ligands [Zn1–O distances from 1.920(3) to 2.461(4) Å, Zn2–O distances from 1.925(3) to 2.325(4) Å], displaying a distorted five-coordinated tetragonal pyramid geometry. As shown in Fig. 3(b) and (c), one carboxylate is in the chelate coordinating mode whereas the other adopts a *syn–anti* bridging mode. As a consequence, the adjacent Zn(II) atoms are bridged by three chadc ligands to result in 1-D double chains along the *a* axis, which are further linked by 3,3′-Hbpt ligands to generated a 2D polymeric coordination layer structure. The Zn···Zn distance separated by the 3,3′-Hbpt linker is 8.791(1) Å, and it is 5.533(1) Å in the dimeric unit bridged by a pair of carboxylate groups.

The structure of **3** is extended into a 3D supramolecular framework by hydrogen-bonding interactions (N4–H4···O3#1, symmetry codes: #1 $-x + 2$, $y + 1/2$, $-z + 3/2$) and $\pi \cdots \pi$ stacking

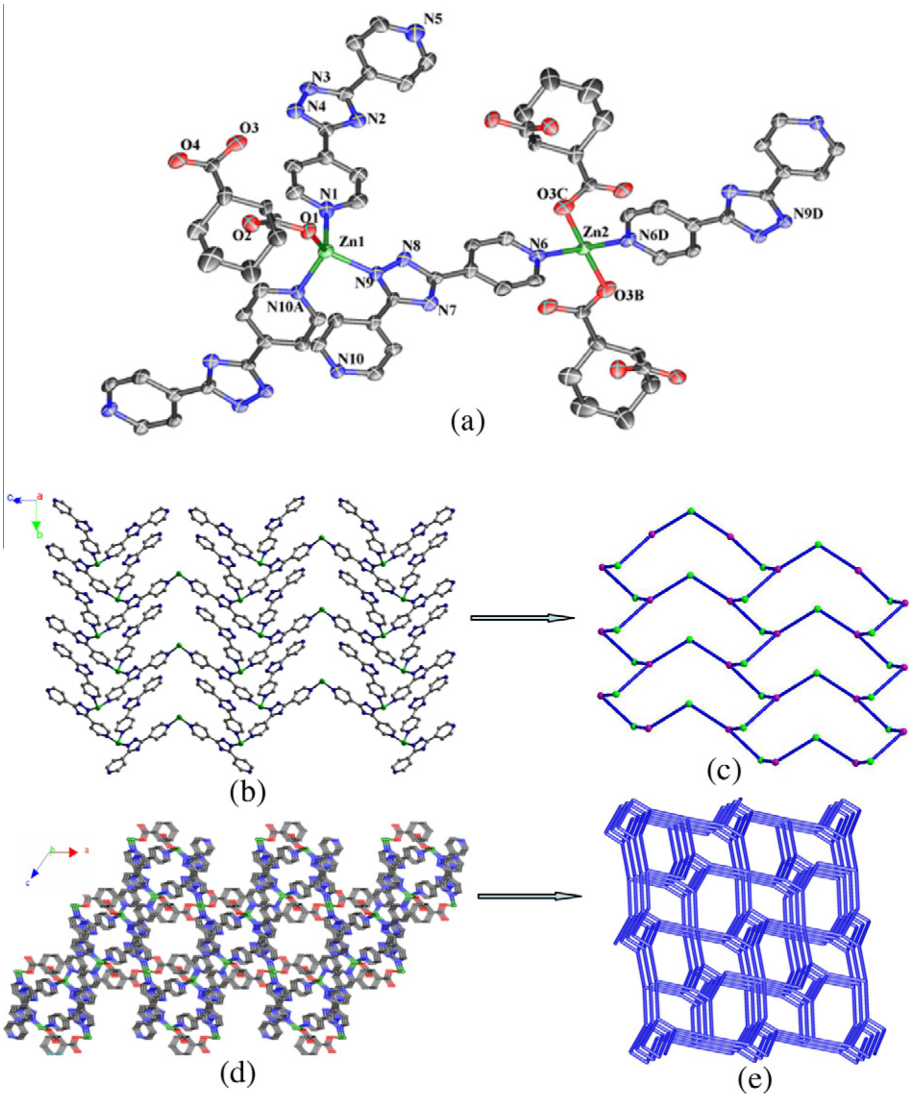

Fig. 2. (a) Structure of **2** showing the local coordination environments of the Zn(II) atoms; (b) view of the 2D network formed by 4,4′-Hbpt and 4,4′-bpt; (c) the simple form of the 2D network; (d) the overall 3D network; (e) schematic representation of the $(6^2.10)_2(6^4.10^2)$ topology of **2**.

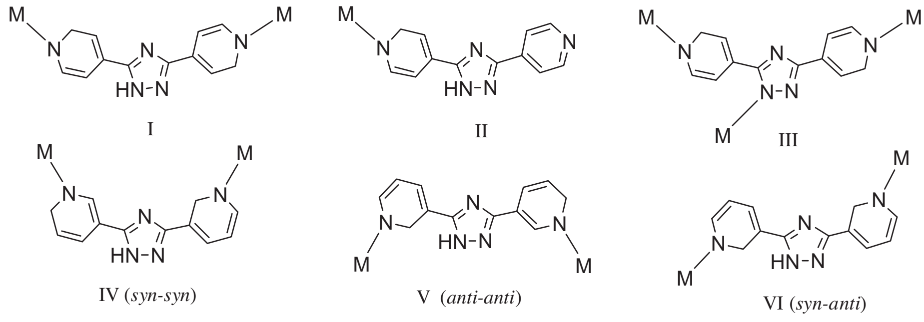

Scheme 1. Primary coordination modes of the 4,4′-Hbpt and 3,3′-Hbpt ligands used in the construction of coordination polymers.

interactions with centroid-to-centroid distances in the range 3.531–3.800 Å. Therefore, hydrogen-bonding interactions and $\pi\cdots\pi$ stacking interactions play important roles in stabilizing the structure. Similar to **3**, the overall 3D supramolecular framework of **4** is generated incorporating N3–H3⋯O3#1, O9–H9A⋯N2 and O9–H9B⋯O6 hydrogen bonding (symmetry codes: #1 $-x+1, -y-1, -z$) and $\pi\cdots\pi$ stacking interactions with centroid-to-centroid distances in the range 3.591–3.745⋯Å (see Fig. 4).

3.2. Photoluminescence properties

Compounds constructed by Zn(II) centers and conjugated organic linkers are promising candidates for photoactive materials with potential applications such as chemical sensors and photochemistry [21,22]. The synthesis of Zn(II) coordination polymers with carefully chosen ligands can be an efficient method for the construction of novel luminescence materials [23–25]. Therefore,

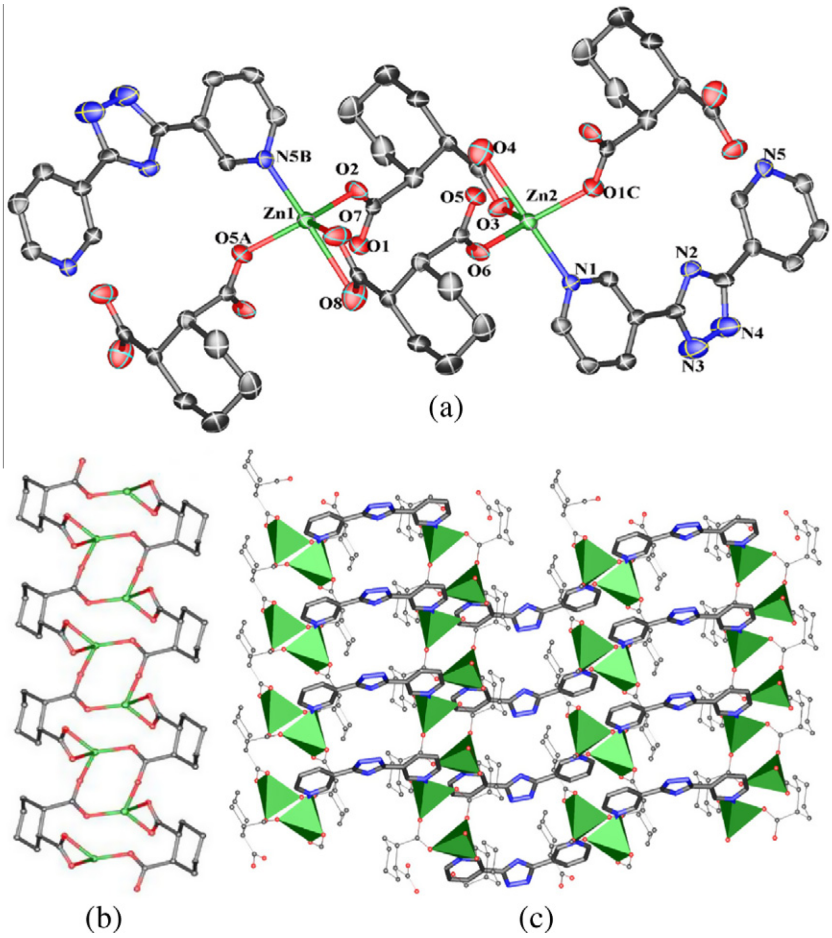

Fig. 3. (a) Structure of **3** showing the local coordination environments of the Zn(II) atoms; (b) the 1-D $[\mathrm{Zn(chadc)}]_n$ chain; (c) the 2-D layer of **3** formed by the $[\mathrm{Zn(chadc)}]_n$ chain and 3,3′-Hbpt connector.

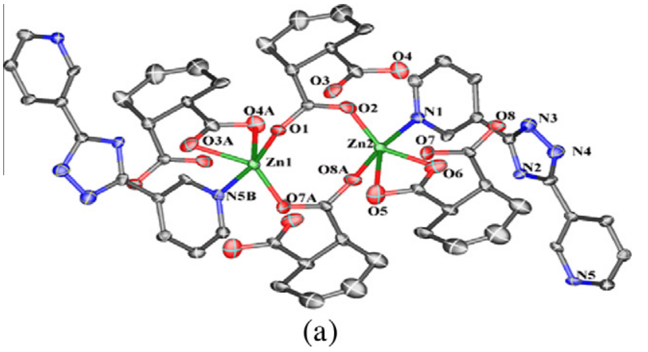

Fig. 4. Structure of **4** showing the local coordination environments of the Zn(II) atoms.

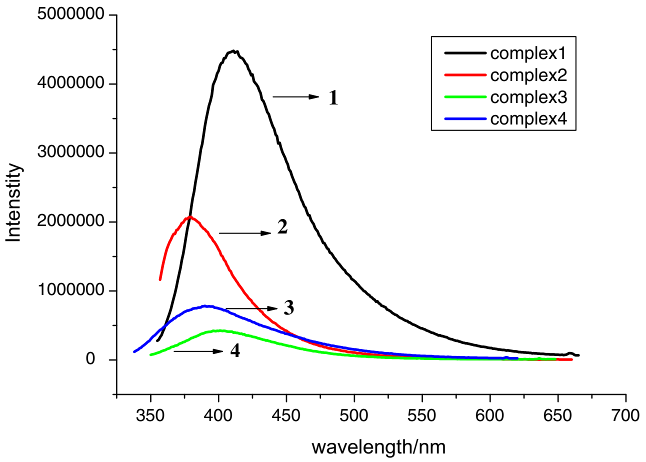

Fig. 5. The solid-state emission spectra of **1**–**4** at room temperature.

the solid-state emission spectra of **1**–**4** have been investigated on crushed single crystals at room temperature, as depicted in Fig. 5. The bpt isomer ligands show very similar emission bands at λ_{max} values of 364 and 368 nm upon excitation at 327 nm, which agree well with our previously reported studies [14]. On complexation of these ligands with Zn(II) atoms, strong luminescence was observable in the solid state at ambient temperature. For complexes **1**–**4**, the maximum emission bands are at 411 ($\lambda_{\mathrm{ex}} = 347$ nm), 379 ($\lambda_{\mathrm{ex}} = 342$ nm), 401 ($\lambda_{\mathrm{ex}} = 335$ nm) and 391 nm ($\lambda_{\mathrm{ex}} = 322$ nm), respectively, which should come from intraligand $\pi \rightarrow \pi*$ transitions [26]. The blue-shift for such fluorescence peaks, compared to that of free bpt isomers, is the result of the incorporation of metal–ligand coordination interactions [14,27]. Furthermore, the enhancements of luminescence may be attributed to the chelating and/or bridging effects of the ligands to the metal centers, which effectively increases the rigidity of the ligands and reduces the loss of energy via radiation less pathways [28].

4. Conclusion

In this work, we have systematically synthesized and characterized four new Zn(II) coordination polymers based on two isomeric ligands, 4,4′-Hbpt and 3,3′-Hbpt, in combination with two similar dicarboxylate ligands. It is evident that the bpt isomers and dicarboxylate ligands have versatile coordination modes to fulfill the diverse network structures. The effect of mixed bpt isomers and similar dicarboxylate ligands on the coordination structure will be further studied in our group and such an investigation may contribute to the development of crystal engineering.

Acknowledgments

We gratefully acknowledge the National Nature Science Foundation of China (Nos. 21061002, 21101035), Guangxi Natural Science Foundation of China (2010GXNSFF013001, 2011GXNSFC018009, 0832098).

Appendix A. Supplementary data

CCDC 852464, 852465, 852466 and 852467 contain the supplementary crystallographic data for complexes **1–4**. These data can be obtained free of charge via http://www.ccdc.cam.ac.uk/conts/retrieving.html, or from the Cambridge Crystallographic Data Centre, 12 Union Road, Cambridge CB2 1EZ, UK; fax: (+44) 1223-336-033; or e-mail: deposit@ccdc.cam.ac.uk.

References

[1] (a) S. Leninger, B. Olenyuk, P. Stang, J. Chem. Rev. 100 (2000) 853;
(b) B. Moulton, M. Zaworotko, J. Chem. Rev. 101 (2001) 1629;
(c) L. Carlucci, G. Ciani, D.M. Proserpio, Coord. Chem. Rev. 246 (2003) 247;
(d) L.G. Beauvais, J.R. Long, Inorg. Chem. 45 (2006) 236;
(e) B.D. Chandler, D.T. Cramb, G.K.H. Shimizu, J. Am. Chem. Soc. 128 (2006) 10403;
(f) Z.-G. Gu, H.-C. Fang, P.-Y. Yin, L. Tong, Y. Ying, S.-J. Hu, W.-S. Li, Y.-P. Cai, Cryst. Growth Des. 11 (2011) 2220.

[2] (a) D.N. Dybtsev, H. Chun, S.H. Yoon, K. Kim, J. Am. Chem. Soc. 126 (2004) 32;
(b) C.N.R. Rao, S. Natarajan, T. Vaidhyanathan, Angew. Chem., Int. Ed. 43 (2004) 1466;
(c) R.J.P. Corriu, A. Mehdi, C. Reye, C. Thieuleux, New J. Chem. 27 (2003) 905;
(d) K.S. Min, M.P. Suh, J. Am. Chem. Soc. 122 (2000) 6834;
(e) S. Kondo, M. Kitagawa, K. Seki, Angew. Chem., Int. Ed. 39 (2000) 2082;
(f) J.-Y. Lee, C.-Y. Chen, H.M. Lee, E. Passaglia, F. Vizza, W. Oberhauser, Cryst. Growth Des. 11 (2011) 1230.

[3] (a) J. Park, S. Hong, D. Moon, M. Park, K. Lee, S. Kang, Y. Zou, R.P. John, G.H. Kim, M.S. Lah, Inorg. Chem. 46 (2007) 10208;
(b) Y. Wang, X.-Q. Zhao, W. Shi, P. Cheng, D.-Z. Liao, S.-P. Yan, Cryst. Growth Des. 9 (2009) 2137;
(c) C.-H. Li, K.-L. Huang, Y.-N. Chi, X. Liu, Z.-G. Han, L. Shen, C.-W. Hu, Inorg. Chem. 48 (2009) 2010.

[4] (a) Y.-L. Wang, D.-Q. Yuan, W.-H. Bi, X. Li, X.-J. Li, F. Li, R. Cao, Cryst. Growth Des. 5 (2005) 1849;
(b) O. Fabelo, J. Pasan, F. Lloret, M. Julve, C.R. Perez, Inorg. Chem. 47 (2008) 3568;
(c) Y.-B. Lu, M.-S. Wang, W.-W. Zhou, G. Xu, G.-C. Guo, J.-S. Huang, Inorg. Chem. 47 (2008) 8935.

[5] (a) B. Zheng, H. Dong, J. Bai, Y. Li, S. Li, M. Scheer, J. Am. Chem. Soc. 130 (2008) 7778;
(b) Y. Tao, J.-R. Li, Q. Yu, W.-C. Song, X.-L. Tong, X.-H. Bu, CrystEngComm 10 (2008) 699.

[6] (a) W.-G. Lu, L. Jiang, X.-L. Feng, T.-B. Lu, Cryst. Growth Des. 8 (2008) 986;
(b) A.-X. Tian, J. Ying, J. Peng, J.-Q. Sha, H.-J. Pang, P.-P. Zhang, Y. Chen, M. Zhu, Z.-M. Su, Inorg. Chem. 48 (2009) 100;
(c) R. Prajapati, L. Mishra, K. Kimura, P. Raghavaiah, Polyhedron 28 (2009) 600.

[7] (a) R. Heck, J. Bacsa, J.E. Warren, M.J. Rosseinsky, D. Bradshaw, CrystEngComm 10 (2008) 1687;
(b) C.-Y. Chen, P.-Y. Cheng, H.-H. Wu, H.M. Lee, Inorg. Chem. 46 (2007) 5691;
(c) L.-L. Qu, Y.-L. Zhu, Y.-Z. Li, H.-B. Du, X.-Z. You, Cryst. Growth Des. 11 (2011) 2444.

[8] (a) M.J. Zaworotko, Nature 451 (2008) 410;
(b) M. Dinca, J.R. Long, Angew. Chem., Int. Ed. 47 (2008) 6766.

[9] (a) S. Kitagawa, R. Matsuda, Coord. Chem. Rev. 251 (2007) 2490;
(b) S. Henke, R.A. Fischer, J. Am. Chem. Soc. 133 (2011) 2064.

[10] (a) H. Arora, F. Lloret, R. Mukherjee, Inorg. Chem. 48 (2009) 1158;
(b) H. Chun, H. Jung, J. Seo, Inorg. Chem. 48 (2009) 2043.

[11] (a) Z. Chang, A.-S. Zhang, T.-L. Hu, X.-H. Bu, Cryst. Growth Des. 9 (2009) 4840;
(b) H. Kumagai, M.A. Tanaka, K. Inoue, K. Takahashi, H. Kobayashi, S. Vilminot, M. Kurmoo, Inorg. Chem. 46 (2007) 5949.

[12] F.-P. Huang, J.-L. Tian, D.-D. Li, G.-J. Chen, W. Gu, S.-P. Yan, X. Liu, D.-Z. Liao, P. Cheng, Inorg. Chem. 49 (2010) 2525.

[13] F.-P. Huang, J.-L. Tian, D.-D. Li, G.-J. Chen, W. Gu, S.-P. Yan, X. Liu, D.-Z. Liao, P. Cheng, CrystEngComm 12 (2010) 395.

[14] (a) F.-P. Huang, J.-L. Tian, G.-J. Chen, D.-D. Li, W. Gu, X. Liu, S.-P. Yan, D.-Z. Liao, P. Cheng, CrystEngComm 12 (2010) 1269;
(b) F.-P. Huang, J.-L. Tian, W. Gu, X. Liu, S.-P. Yan, D.-Z. Liao, P. Cheng, Cryst. Growth Des. 10 (2010) 1145;
(c) F.-P. Huang, J.-L. Tian, W. Gu, S.-P. Yan, Inorg. Chem. Commun. 13 (2010) 90;
(d) F.-P. Huang, H.-D. Bian, Q. Yu, J.-L. Tian, H. Liang, S.-P. Yan, D.-Z. Liao, P. Cheng, CrystEngComm (2011), doi:10.1029/c1ce05562c.

[15] N.N. Vyatsheslav, V.Z. Nikolay, Z.V. Sergey, ARKIVOC (2005) 118.

[16] G.M. Sheldrick, Acta Crystallogr. A46 (1990) 467.

[17] G.M. Sheldrick, SHELXL97, Program for X-ray Crystal Structure Solution, University of Göttingen, Göttingen, Germany, 1997.

[18] A.F. Wells, Three-Dimensional Nets and Polyhedra, Wiley-Interscience, New York, 1977.

[19] (a) V.A. Blatov, A.P. Shevchenko, V.N. Serezhkin, J. Appl. Crystallogr. 33 (2000) 1193;
(b) G.A. Farnum, R.L. LaDuca, Cryst. Growth Des. 11 (2010) 1897.

[20] K.M. Blake, J.S. Lucas, R.L. LaDuca, Cryst. Growth Des. 11 (2011) 1287.

[21] G.D. Santis, L. Fabbrizzi, M. Licchelli, A. Poggi, A. Taglietti, Angew. Chem., Int. Ed. Engl. 35 (1996) 202.

[22] (a) Q. Wu, M. Esteghamatian, N.-X. Hu, G. Enright, Y. Tao, M. Díorio, S. Wang, Chem. Mater. 12 (2000) 79;
(b) J.E. McGarrah, Y.J. Kim, M. Hissler, R. Eisenberg, Inorg. Chem. 40 (2001) 4510.

[23] D. Tanaka, S. Horike, S. Kitagawa, M. Ohba, M. Hasegawa, Y. Ozawa, K. Toriumi, Chem. Commun. (2007) 3142.

[24] (a) E. Cariati, X. Bu, P.C. Ford, Chem. Mater. 12 (2000) 3385;
(b) F. Wurthner, A. Sautter, Chem. Commun. (2000) 445;
(c) D.M. Ciurtin, N.G. Pschirer, M.D. Smith, U.H.F. Bunz, Chem. Mater. 13 (2001) 2743;
(d) Y.-B. Dong, H.-Y. Wang, J.-P. Ma, D.-Z. Shen, R.-Q. Huang, Inorg. Chem. 44 (2005) 4679.

[25] (a) S.-L. Zheng, X.-M. Chen, Aust. J. Chem. 57 (2004) 703;
(b) S.-L. Zheng, J.-H. Yang, X.-L. Yu, X.M. Chen, W.-T. Wong, Inorg. Chem. 43 (2004) 830;
(c) M. Du, X.-J. Jiang, X.-J. Zhao, Inorg. Chem. 46 (2007) 3984.

[26] S.-M. Fang, Q. Zhang, M. Hu, X.-G. Yang, L.-M. Zhou, M. Du, C.-S. Liu, Cryst. Growth Des. 10 (2010) 4773.

[27] M. Du, X.-J. Jiang, X.-J. Zhao, Inorg. Chem. 45 (2006) 3998.

[28] (a) B. Valeur, Molecular Fluorescence: Principles and Applications, Wiley-VCH, 2002;
(b) J.-J. Wang, C.-S. Liu, T.-L. Hu, Z. Chang, C.-Y. Li, L.-F. Yan, P.-Q. Chen, X.-H. Bu, Q. Wu, L.-J. Zhao, Z. Wang, X.-Z. Zhang, CrystEngComm 10 (2008) 681.